



## **Time-course of myelination and atrophy on cerebral imaging in 35 patients with PLP1 -related disorders**

Catherine Sarret, Jean-Jacques Lemaire, Davide Tonduti, Anna Sontheimer, Jérôme Coste, Bruno Pereira, Fabien Feschet, Basile Roche, Odile Boespflug-Tanguy

### **► To cite this version:**

Catherine Sarret, Jean-Jacques Lemaire, Davide Tonduti, Anna Sontheimer, Jérôme Coste, et al.. Time-course of myelination and atrophy on cerebral imaging in 35 patients with PLP1 -related disorders. *Developmental Medicine and Child Neurology*, 2016, 58 (7), pp.706-713. 10.1111/dmcn.13025 . hal-01654750

**HAL Id: hal-01654750**

**<https://uca.hal.science/hal-01654750>**

Submitted on 7 Dec 2018

**HAL** is a multi-disciplinary open access archive for the deposit and dissemination of scientific research documents, whether they are published or not. The documents may come from teaching and research institutions in France or abroad, or from public or private research centers.

L'archive ouverte pluridisciplinaire **HAL**, est destinée au dépôt et à la diffusion de documents scientifiques de niveau recherche, publiés ou non, émanant des établissements d'enseignement et de recherche français ou étrangers, des laboratoires publics ou privés.

# Time-course of myelination and atrophy on cerebral imaging in 35 patients with PLP1-related disorders

Catherine SARRET<sup>1,2</sup>, Jean-Jacques LEMAIRE<sup>1,3</sup>, Davide TONDUTI<sup>4,5</sup>,  
Anna SONTHEIMER<sup>1</sup>, Jérôme COSTE<sup>1</sup>, Bruno PEREIRA<sup>1,6</sup>, Fabien FESCHET<sup>1</sup>,  
Basile ROCHE<sup>1</sup> et Odile BOESPFLUG-TANGUY<sup>4,7</sup>

1 Image-Guided Clinical Neuroscience and Connectomics (IGCNC), Clermont University, University of Auvergne;

2 Department of Paediatrics, Clermont-Ferrand, University Hospital;

3 Department of Neurosurgery, Clermont-Ferrand University Hospital, Clermont-Ferrand;

4 Inserm U1141 Paris Diderot Sorbonne University–Paris, Cite DHU PROTECT, Robert Debre Hospital, Paris, France.

5 Department of Child Neurology, Neurological Institute C. Besta Foundation IRCCS, Milan, Italy.

6 Biostatistics Unit (DRCI), Clermont-Ferrand University Hospital, Clermont-Ferrand;

7 Department of Child Neurology and Metabolic Diseases; Leukodystrophies Reference Centre, Robert Debre Hospital, Paris, France.

Correspondence to Catherine Sarret at IGCNC, EA7282, Clermont-Ferrand University Hospital, 58 rue Montalembert, 63003 Clermont-Ferrand Cedex, France.

E-mail: csarret@chu-clermontferrand.fr.

**Aim:** Brain magnetic resonance imaging (MRI) motor development score (MDS) correlations were used to analyze the natural time-course of hypomyelinating PLP1-related disorders (Pelizaeus-Merzbacher disease [PMD] and spastic paraplegia type 2).

**Method:** Thirty-five male patients (ranging from 0.7–43.5y at the first MRI) with PLP1-related disorder were prospectively followed over 7 years. Patients were classified according to best motor function acquired before 5 years (MDS) into five categories (from PMD0 without motor acquisition to PMD4 with autonomous walking). We determined myelination and atrophy scores and measured corpus callosum area, volume of cerebellum, white matter and grey matter on 63 MRI.

**Results:** Age-adjusted multivariate analysis revealed that patients with PMD0-1 had higher severity atrophy scores and smaller corpus callosum area than did patients with PMD2 and PMD3-4. Myelination score increased until 12 years. There was evidence that the mean myelination differed in frontal white matter, arcuate fibres, and internal capsules among the groups. Most patients showed worsening atrophy (brain, cerebellum, corpus callosum), whereas grey matter and white matter proportions did not change.

**Interpretation:** Brain atrophy and myelination of anterior cerebral regions appear to be pertinent biomarkers of motor development. The time-course of inter- and intra-individual cerebral white matter and grey matter atrophy suggests that both oligodendrocytes and neurons are involved in the physiopathology of PLP1-related disorders

## INTRODUCTION

Pelizaeus-Merzbacher disease (PMD; OMIM 312080) and spastic paraplegia type 2 (SPG2; OMIM 312920) are prototypic inherited defects of central nervous system (CNS) myelin formation. This X-linked form of hypomyelinating leukodystrophy (HLD1, OMIM 312080) is caused by mutations of the proteolipid protein 1 gene (PLP1), which encodes the two major myelin proteins of the CNS, PLP and its spliced isoform DM20 in oligodendrocytes. The clinical findings associated with PLP1 mutations span a wide-spectrum continuum extending from severe congenital PMD forms to relatively mild late-onset SPG2 leading to the concept of PLP1-related disorders.<sup>1</sup>

PMD in males is characterized by early (<6mo) impairment of psychomotor development. In the first years of active myelination, hypotonia is associated with neurological signs gradually modifying as the CNS matures (nystagmus, choreoathetotic movements, ataxia). The large majority of patients improve during childhood. We classify them according to the best motor function achieved between the ages of 2 years and 5 years (motor developmental score, MDS) to demonstrate a genotype-phenotype correlation.<sup>1</sup> PMD1 (head control) and PMD2 (sitting position) are the most common forms and are usually associated with PLP1 duplications. Missense mutations are rare but usually cause the most severe forms without motor acquisitions and dystonia (PMD0 form, also named 'congenital' forms). PLP1 loss-of-function (null mutations and large deletions) leads to the mildest PMD3/PMD4 (or SPG2) forms with acquisition of walking capacities with/ without aid. Cognitive and behavioural development is also better preserved in mild forms.

The defect in CNS myelin formation is demonstrated by both dramatic and extensive abnormalities of multimodal evoked potentials in the CNS and a diffuse hypomyelinated pattern of the supratentorial white matter on magnetic resonance imaging (MRI).<sup>2</sup> This 'hypomyelinated' pattern is characterized by a diffuse hypersignal of the white matter on T2-weighted and fluid-attenuated inversion recovery (FLAIR) sequences contrasting with a normal hypersignal or isosignal on T1-weighted sequences in comparison with grey matter. Clinical severity appears to correlate with degree of hypomyelination, and slow progression of myelination has been reported in the youngest patients.<sup>3–6</sup> In parallel, local improvement of myelination was reported on MRIs of two out of four children classified with severe PMD after intra-cerebral grafting of neural stem cells, particularly at injection points.<sup>7</sup>

Progressive spastic paraplegia with pyramidal tract signs is subsequently observed in patients with both PMD and SPG2, leading to severe quadriplegia, amyotrophia, and optic atrophy at the end of the second–fourth decade and accompanied by the development of cortico-

subcortical atrophy on MRI and late cognitive decline.<sup>8</sup> A recent large series of 50 males with PMD/SPG2 and 11 heterozygous females found a correlation between clinical severity and white matter atrophy of the whole brain and corpus callosum.<sup>9</sup>

However, there is still a dearth of MRI data on the natural time-course of PMD/SPG2. To address this gap, we set out to identify pertinent MRI biomarkers of disease evolution, through a prospective analysis of clinical exams and MRIs of 35 PLP1-mutated males with variable forms of PMD/SPG2, followed over 7 years.

## **METHOD**

### **Patients**

Thirty-five males from 32 families with PLP1 mutations were enrolled from January 2002 to December 2009 for prospective follow-up. MDS was determined according to the best motor development observed between 2 years and 5 years, adapted from Cailloux et al. and Inoue, as: no motor acquisition (PMD0), only head control (PMD1), sitting (PMD2), walking with aid (PMD3), or autonomous walking (PMD4).<sup>1,10</sup> Clinical follow-up was carried out by an experienced neuropaediatrician (OB-T) at each visit to our medical centre. All patients had at least one MRI (named MRI-1), and 17 patients had repeat MRIs (nine patients twice, five patients three times, and three patients four times) at a minimal interval of 1 year using the same MRI protocol at the same medical centre.

### **MRI data, image processing, and biomarkers**

Images were acquired on a 1.5-Tesla Siemens MR scanner, as follows: axial, sagittal, and coronal slices; T1-weighted, T2-weighted, and FLAIR sequences (Fig. 1). Anonymized series were co-registered and aligned with the anterior commissure-posterior commissure (ACPC) line (Iplan 3.0; Brainlab, Feldkirchen, Germany). Biomarkers explored across MRI data were atrophy and myelination scores, quantitative evaluation of corpus callosum area, volumes of cerebellum and white matter/grey matter compartments.

*Atrophy and myelination scores:* Myelination score (Table I) was determined by an adaptation of Plecko et al.'s scheme.<sup>6</sup> White matter signal was qualified in different regions-of-interest as hyper-, iso-, or hypointense compared with grey matter signal, on T1-weighted, T2weighted, and FLAIR images. Myelination scores were determined from all MRI and expressed as percentage of expected myelination according to age. Atrophy score (Table I) is a semi-

quantitative score obtained on classical MRI interpretation by radiologists. To limit subjectivity in interpretation, the atrophy scores were determined in a blind way by two neuropaediatricians (CS and DT).

*CNS segmentation, surface and volume measurements:* These were performed using Iplan 3.0 on FLAIR slices as white matter-grey matter signal contrast was visually maximal. Corpus callosum and cerebellum segmentation was determined manually (Fig. 1). Total intracranial volume (TIV) was determined instead of strict brain volume to take into account the brain growth in young patients and the predictable white as well as grey matter atrophy. TIV, white matter and grey matter compartments were determined and extracted automatically (Statistical Parametric Mapping 8, Wellcome Trust Centre for Neuroimaging, London, UK; Matlab 7.0, Mathworks, Sherborn, MA, USA). Grey matter and white matter maps (dicomizer AVIZO software, Visualization Sciences Group, FEI, US) were co-registered with ACPC-aligned MRI series. Corpus callosum area/TIV ratio, cerebellum volume/TIV ratio, white matter compartment/ TIV ratio and grey matter compartment/TIV ratio were calculated, to account for brain growth over time.

## **Statistical analysis**

Statistical analysis was performed using Stata 13 (StataCorp, College Station, TX, USA). The tests were twosided, with a type-I error set at  $\alpha=0.05$ . Quantitative data, expressed as mean and standard deviation or median and interquartile range according to statistical distribution, were compared between independent groups (PMD0-1, PMD2, and PMD3-4) using a Kruskal–Wallis test followed by the appropriate post-hoc Dunn’s test. An ANCOVA (analysis of covariance) was performed with age as the adjustment covariate. The assumption of the normality of residuals was also studied using the Shapiro–Wilk test. Our data not exhibiting normal distributions, a log-transformation was proposed to achieve normality of several variables and to allow the correct use of these analyses. As proposed by some statisticians, we chose to report all the individual p-values without doing any mathematical correction for distinct tests comparing groups.<sup>11</sup> A particular focus was given to the magnitude of improvement and to the clinical relevance.<sup>12</sup>

A longitudinal descriptive survey was led over a maximum of 7 years according to availability of MRI and biomarker data.

The study secured written informed consent from all parents and was approved by the relevant French institutional review boards (CPP Sud-Est VI No. AU788, CNIL No. 1406552, AFSSAPS No. B90298-60).

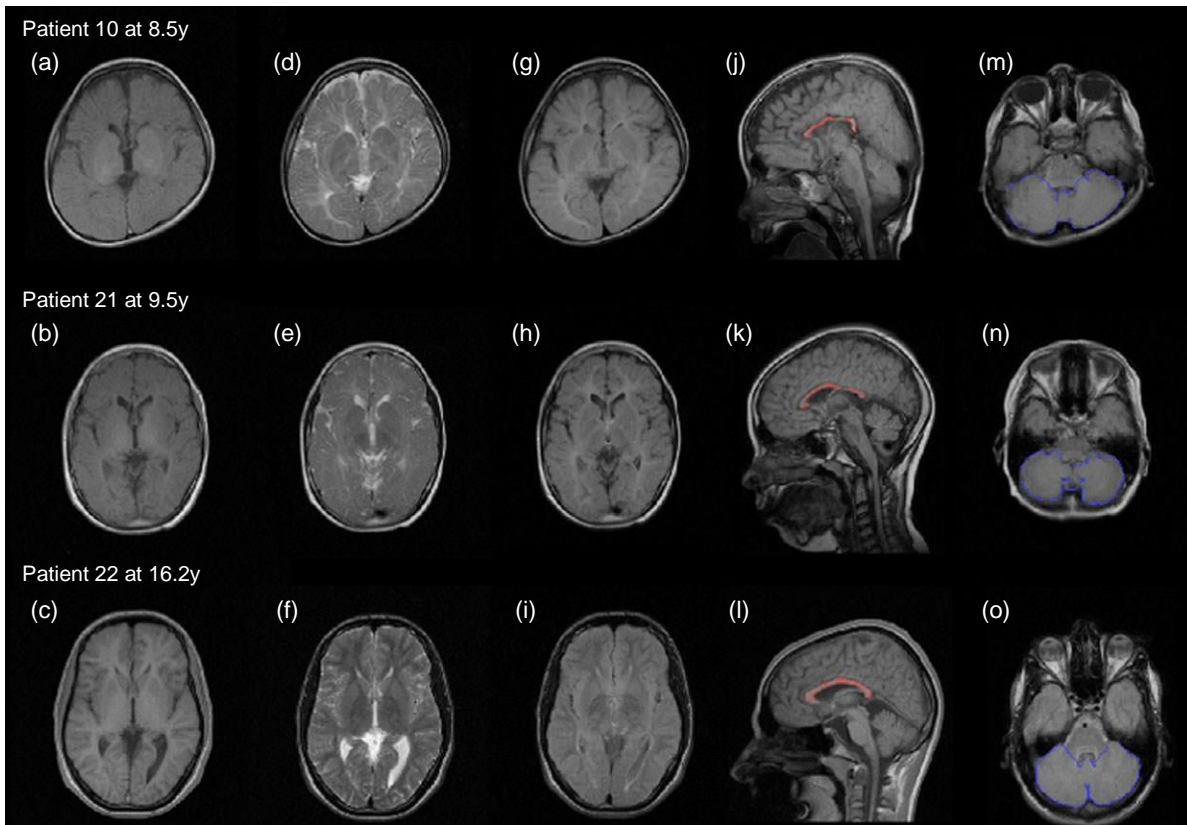


**Figure 1:** Magnetic resonance imaging of patients with Pelizaeus-Merzbacher disease (PMD)/spastic paraplegia type 2 (SPG2); severe (PMD0; top row), intermediate (PMD2; intermediate row), and mild (PMD4; bottom row) forms. T1-weighted (a–c), T2-weighted (d–f), and fluid-attenuated inversion recovery (FLAIR) (g–i) axial slices, anterior commissure-posterior commissure aligned, showing different degrees of hypomyelination according to motor development score. Corpus callosum manual segmentation on midline FLAIR (j–k) and T1-weighted (l) sagittal slices. Manual segmentation of cerebellum on FLAIR axial slices (m–o) through the middle cerebellar peduncle.

## RESULTS

Table II summarizes patient MDS, genotype, and age at MRI acquisition. The population consisted of 19 duplicated patients and 16 patients with point mutation (Table II). In total, we had 63 structural MRI available in 35 patients. Mean age at MRI-1 was 11.77.8 years (median 10.9y; range 0.7–43.5y). Table III gives mean and median ages in each group.

### Myelination and atrophy scores

Myelination (on 62 MRIs) and atrophy scores (on 63 MRIs) were calculated from 35 patients.

The results of 35 MRI-1 were analyzed according to MDS using three groups PMD0-1, PMD2, and PMD3-4. There was no evidence of a difference in mean gross total myelination scores between the three groups, whereas the mean atrophy scores were more severe in



patients with PMD0-1 than in patients with PMD2 and PMD3-4 (PMD2,  $p=0.033$ ; PMD3-4,  $p=0.040$ ) (Table III).

Table I: Atrophy and myelination scoring

Atrophy score		Myelination score			
CNS regions and characterization		CNS regions			
Corpus callosum atrophy		Subcortical white matter (Arcuate fibres)			
Lobar (deep) white matter atrophy		Lobar (deep) white matter		Frontal	
Lateral ventricle enlargement				Temporal	
Subarachnoid space enlargement				Parietal	
Cerebellar hemisphere atrophy				Occipital	
Pons atrophy		Corpus callosum			
Fourth ventricle enlargement		Internal capsule		Anterior limb Posterior limb	
		Cerebellar white matter			
		Pons			
Quantitative score for each region		Quantitative score for each region			
No atrophy or enlargement	0	Characterization of white matter signal versus grey matter signal			
Moderate atrophy or enlargement	1	T1-weighted	T2-weighted	FLAIR	
Intermediate atrophy or enlargement	2	hypo	hyper	hyper	0
Severe atrophy or enlargement	3	iso	hyper	hyper	1
		hyper	hyper	hyper	2
		hyper	iso	hyper	3
		hyper	hypo	hyper	4
		hyper	hypo	iso	5
		hyper	hypo	hypo	6
Total score		Total score			
Minimal score (no atrophy)	0	Minimal score (no myelination)			0
Maximal score (maximal atrophy)	21	Maximal score (achieved myelination)			60

*CNS, central nervous system; FLAIR, fluid-attenuated inversion recovery.*

Analysis led on the subgroup of 17 patients who had successive MRIs revealed that atrophy scores increased over time in 82% of patients (14/17) (Fig. 2a). Progressive atrophy was never observed before 5 years and was only present between 5 years and 7 years in two patients with PMD2 and one patient with PMD3. For the remaining patients, atrophy increased by 8.72% between 10 years and 20 years. In contrast, total myelination score clearly improved for 7/17 patients after the expected age of 2 years of complete myelination in normal children (Fig. 2b). This increase was observed in the four patients with PMD2 and one patient with

PMD3 analysed between 3 years and 7 years, but also for two patients (one PMD2 and one PMD3) between 7 years and 12 years. In the 10 remaining patients analysed after 7 years, myelination score remained stable except in one patient with PMD3 whose myelination score decreased during adolescence over a period of 6.5 years. Inter-individual variability was particularly visible in the PMD3-4 group (10 patients).

Table II: List of patients and families with Pelizaeus-Merzbacher disease (PMD)/spastic paraplegia type 2

Patient	Family	MDS	Age at MRI (y)	PLP1 mutation	Deduced protein	Family genetic number
1	1	PMD2	16.8/19.1	c.608A>G	p.Asp202Gly	37
2	2	PMD2	4.5/7.5	c.659G>A	p.Cys220Tyr	759
3	3	PMD2	8.8	Duplication	Overexpression	81
4	4	PMD2	6.2	c.125delG	p.Gly42AlafsX5	1038
5	5	PMD0	13.8/17.4	c.454-1G>T	p.Phe117ValfsX27 p.117_150del p.152_185del	26
6	6	PMD2	13.6	Duplication	Overexpression	154
7	7	PMD3	11.0/14.5/16.2/17.4	c.307delG	p.Asp103ThrfsX11	905
8	7	PMD3	13.6/17.2/18.8/20.1	c.307delG	p.Asp103ThrfsX11	905
9	8	PMD3	32.8	c.173A>G	p.Tyr58X	106
10	9	PMD0	8.5/11.0	Duplication	Overexpression	545
11	10	PMD3	5.3/6.4/8.3/11.5	Duplication	Overexpression	407
12	11	PMD2	2.8/5.7/7.8	Duplication	Overexpression	887
13	12	PMD0	8.6	c.670C>T	p.Leu224Phe	766
14	13	PMD2	17.0	Duplication	Overexpression	28
15	14	PMD1	10.5/15	Duplication	Overexpression	150
16	15	PMD0	11.5	Duplication	Overexpression	42
17	16	PMD2	14.8	Duplication	Overexpression	61
18	17	PMD2	21.8	c.646C>T	p.Pro216Ser	24
19	18	PMD3	3.7/5.5	Duplication	Overexpression	1114
20	19	PMD3	12.3/19.0	c.646C>G	p.Pro216Ala	53
21	20	PMD3	9.5/11.5/13.5/16.2	Duplication	Overexpression	46
22	21	PMD4	16.2	c.548C>A	p.Thr183Asn	41
23	22	PMD2	0.7/4.4/6.8	Duplication	Overexpression	1059
24	23	PMD2	2.3	Duplication	Overexpression	1910
25	24	PMD0	3.0	c. 454-1G>A	p.Phe117ValfsX27 p.117_150del p.117_157del	767
26	25	PMD2	8.6/11.1/12.7	Duplication	Overexpression	418
27	26	PMD2	5.8	Duplication	Overexpression	1201
28	2	PMD2	43.5	c.659G>A	p.Cys220Tyr	759
29	27	PMD2	4.3	Duplication	Overexpression	1251
30	28	PMD4	37.0/41.0	c.801G>T	p.Val219Phe	1
31	29	PMD2	5.1	Duplication	Overexpression	1026
32	8	PMD3	8.4/10.8/13.3/14.4	c.173A>G	p.Tyr58X	106
33	30	PMD1	3.5	c.327delC	p.Cys109TrpfsX11	1171
34	31	PMD1	8.6	Duplication	Overexpression	1776
35	32	PMD1	5.7	Duplication	Overexpression	968

*Motor developmental score (MDS), age (y) at magnetic resonance imaging (MRI), genotype (at the DNA level) and deduced protein. Family genetic number corresponds to our laboratory family number and refers to previous publication.<sup>1</sup>*

We then considered the myelination score of the 10 individual white matter regions determined at MRI-1 in the different groups of patients. After adjusting for age, there was evidence that the mean myelination differed in only three regions. The frontal white matter



( $p=0.029$ ) and anterior limb of the internal capsule ( $p=0.045$ ) appeared less achieved in patients with PMD0-1 than patients with PMD3-4. Myelination of arcuate fibres (U fibres) was less achieved in patients with PMD0-1 ( $p=0.046$ ) and PMD2 ( $p=0.045$ ) than in patients with PMD3-4 (Table III) despite very poor U-fibre myelination scores in all groups. Interindividual variability in the regional myelination scores was particularly visible in the PMD3-4 group.

These results showed that in PLP1-related disorders, the MDS that we had previously used to demonstrate a genotype-phenotype correlation is strongly correlated with the MRI atrophy score used here. Myelination scores for frontal white matter and to a lesser extent the anterior limb of the internal capsule and U-fibres partially segregated the different severity groups. Follow-up MRIs performed in 50% of our 35 patients demonstrated that myelination scores can improve actively between 3 years and 7 years and more rarely and to a lesser extent between 7 years and at least 12 years. During adolescence, myelination scores remain stable whereas atrophy scores clearly increase. We then quantified different white matter and grey matter structures to better assess this atrophic process.

### **Quantification of white matter and grey matter structures**

We first quantified the area/volume ratios of two structures known to change during the active phase of myelin development: the corpus callosum, a pure white matter structure, and the cerebellum including white matter and grey matter (Fig. 1). Considering the 35 MRI-1, we found that mean corpus callosum area/TIV ratio was statistically smaller in patients with PMD0-1 than in patients with PMD3-4 after adjustment for age ( $p=0.017$ ; Table III). However, both corpus callosum area/TIV ratio and cerebellum volume/TIV ratio decreased in 88% ( $n=15$ ) and 76% ( $n=13$ ), respectively, of the 17 patients that underwent successive MRI (Fig. 2c, d).

Automated segmentation of white matter and grey matter on FLAIR sequences was effective for 27 MRI in 22 patients, including all groups of patients. There was no evidence of a difference in mean white matter and grey matter compartments between the different severity groups (Table III). The grey matter compartment was usually twice as large as the white matter compartment. Two successive MRIs were interpretable in 5/22 analyzable patients. White matter and grey matter compartments remained stable over time except in two patients (one patient with PMD0 and one patient with PMD2) who underwent two successive MRI at adolescence, in whom white matter compartment/TIV ratio decreased.

These results suggest that in PLP1-mutated patients, corpus callosum area, but not its myelination level, is correlated with severity of impairment of motor milestones. Interestingly, cerebellum atrophy tends to occur over time in parallel with the corpus callosum atrophy,

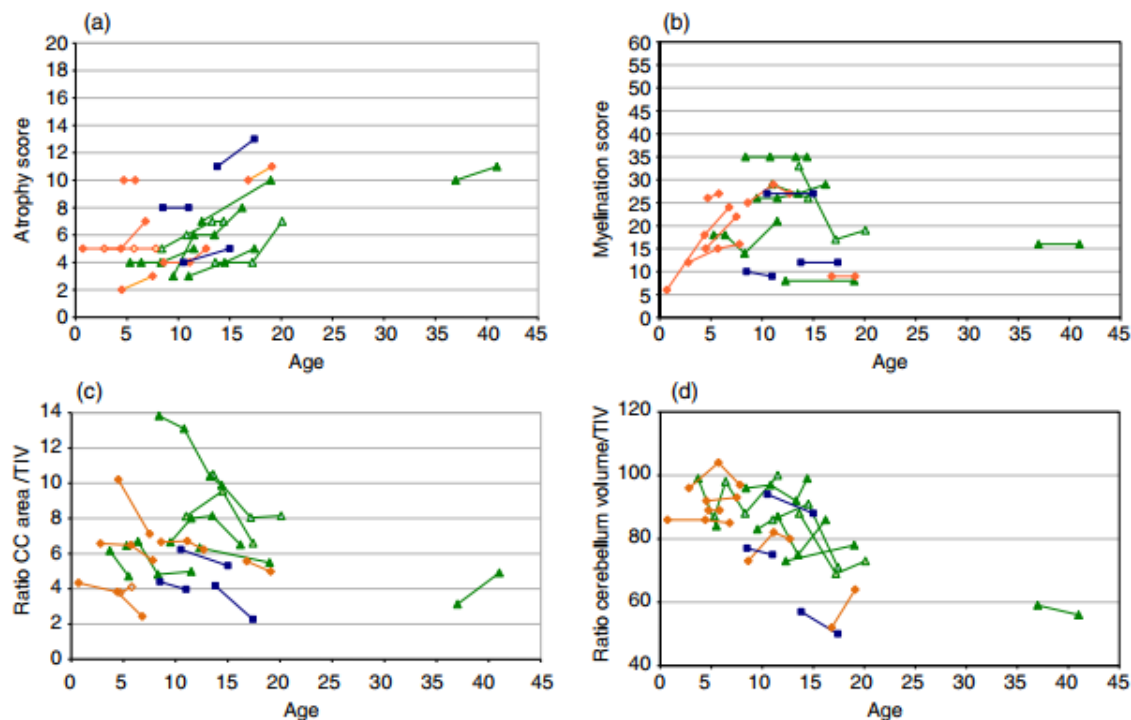
whereas the white matter compartment, despite its severe defect, tends to remain stable compared to the grey matter compartment, at least until adolescence.

Table III: Results of statistical analyses for the different biomarkers

	PMD0–1	PMD2	PMD3–4	Omnibus p-value
Number of patients	9	16	10	
Mean age in years (SD)	8.19 (3.59)	10.96 (10.67)	14.98 (11.17)	0.29
Median age in years (interquartile range)	8.60 (4.8)	7.4 (11–4)	11.65 (7–8)	
Percentage of myelination score according to age <sup>a</sup>	29.44 (16.27)	35.12 (12.98)	41.40 (20.91)	0.36
Versus PMD0-1 (p-value)		0.366	0.074	
Versus PMD2 (p-value)			0.290	
Atrophy score <sup>a</sup>	7.77 (4.06)	5.62 (3.99)	6.50 (4.48)	0.34
Versus PMD0-1 (p-value)		0.033	0.040	
Versus PMD2 (p-value)			0.830	
Corpus callosum area/TIV (10 <sup>4</sup> ) <sup>a</sup>	5.36 (2.11)	6.50 (2.22)	7.31 (3.05)	0.11
Versus PMD0-1 (p-value)		0.136	0.017	
Versus PMD2 (p-value)			0.180	
Cerebellum volume/TIV (10 <sup>2</sup> ) <sup>a</sup>	8.14 (1.19)	8.06 (1.54)	8.17 (1.22)	0.98
Versus PMD0-1 (p-value)		0.650	0.145	
Versus PMD2 (p-value)			0.210	
Percentage of expected myelination – frontal white matter <sup>a</sup>	15.89 (18.69)	24.93 (24.26)	36.60 (29.17)	0.16
Versus PMD0-1 (p-value)		0.270	0.029	
Versus PMD2 (p-value)			0.140	
Percentage of expected myelination – temporal white matter <sup>a</sup>	24.11 (14.54)	32.25 (20.50)	40.00 (25.02)	0.25
Versus PMD0-1 (p-value)		0.281	0.060	
Versus PMD2 (p-value)			0.260	
Percentage of expected myelination – parietal white matter <sup>a</sup>	29.44 (7.06)	33.13 (20.15)	31.60 (12.14)	0.92
Versus PMD0-1 (p-value)		0.491	0.566	
Versus PMD2 (p-value)			0.970	
Percentage of expected myelination – occipital white matter <sup>a</sup>	20.22 (16.02)	26.94 (24.18)	31.40 (22.74)	0.50
Versus PMD0-1 (p-value)		0.326	0.113	
Versus PMD2 (p-value)			0.390	

Percentage of expected myelination – arcuate fibres <sup>a</sup>	1.00 (1.00)	1.06 (0.85)	2.10 (1.73)	0.16
Versus PMD0-1 (p-value)		0.840	0.046	
Versus PMD2 (p-value)			0.035	
Percentage of expected myelination – ant limb internal capsule <sup>a</sup>	24.22 (11.89)	32.44 (16.46)	43.40 (24.99)	0.13
Versus PMD0-1 (p-value)		0.318	0.045	
Versus PMD2 (p-value)			0.180	
Percentage of expected myelination – post limb internal capsule <sup>a</sup>	35.00 (35.74)	35.25 (19.26)	38.10 (22.32)	0.83
Versus PMD0-1 (p-value)		0.985	0.808	
Versus PMD2 (p-value)			0.790	
Percentage of expected myelination – corpus callosum <sup>a</sup>	31.56 (25.43)	44.81 (24.04)	45.10 (26.04)	0.33
Versus PMD0-1 (p-value)		0.225	0.276	
Versus PMD2 (p-value)			0.980	
Percentage of expected myelination – cerebellar white matter <sup>a</sup>	31.67 (17.39)	50.00 (30.16)	45.10 (33.14)	0.36
Versus PMD0-1 (p-value)		0.081	0.146	
Versus PMD2 (p-value)			0.910	
Percentage of expected myelination – pons white matter <sup>a</sup>	64.78 (35.67)	70.75 (26.11)	68.20 (31.84)	0.96
Versus PMD0-1 (p-value)		0.638	0.793	
Versus PMD2 (p-value)			0.860	
Sample size for grey matter and white matter evaluation	3	11	3	
Grey matter compartment/TIV <sup>a</sup>	0.41 (0.12)	0.36 (0.04)	0.42 (0.14)	0.74
Versus PMD0-1 (p-value)		0.349	0.826	
Versus PMD2 (p-value)			0.240	
White matter compartment/TIV <sup>a</sup>	0.19 (0.06)	0.17 (0.03)	0.24 (0.11)	0.55
Versus PMD0-1 (p-value)		0.621	0.297	
Versus PMD2 (p-value)			0.070	

<sup>a</sup> Results are expressed as mean values (SD); bold face for  $p < 0.05$ ; ant, anterior; post, posterior. Omnibus p-value obtained without age adjustment (Kruskal–Wallis test) whereas other p-values were performed using ANCOVA (analysis of covariance) with age as the adjustment covariate. Effect sizes with 95% confidence interval are given in Table SI. PMD, Pelizaeus-Merzbacher disease; TIV, total intracranial volume.



**Figure 2:** Inter- and intra-individual magnetic resonance imaging (MRI) evolution over time in the subgroup of 17 patients with successive MRIs. Atrophy scores (a; y-axis; from 0, no atrophy, to 21, maximal atrophy) and myelination score (b; y-axis; from 0, no myelination to 60, achieved myelination) according to age (x-axis; years); atrophy tends to increase over time, and myelination tends to increase until 12 years before stabilizing as patients get older. Corpus callosum area/total intracranial volume (TIV) ratios (c; y-axis) according to the age (x-axis; years); note inter- and intra-individual progressive corpus callosum atrophy over time. Cerebellum volume/TIV ratios (d; y-axis) according to age (x-axis; years); note inter- and intra-individual progressive cerebellum atrophy over time. Blue squares: Pelizaeus-Merzbacher disease (PMD)0-1 orange diamonds: PMD2; green triangles: PMD3-4.

Several patients are represented with empty symbols for visibility.

## DISCUSSION

We analyzed cerebral MRIs performed at the same medical centre at a mean age of 12 years on a large cohort of PLP1-mutated male patients. The 35 patients included were representative of the broad clinical spectrum of severity usually described in the PMD/SPG2 phenotype. We used MDS that we had previously demonstrated to correlate to the genotype.<sup>1</sup> MRI follow-up was possible in half of them, with 45 successive MRIs.

Our results show that MDS is more correlated to gross atrophy score than to gross myelination score. Looking at the frontal and anterior capsule, atrophy score seems to increase over time, which is consistent with results from a small series of patients with PMD,<sup>13,14</sup> as well as a recent large series made up of male patients with PMD and

pauci-symptomatic heterozygous females.<sup>9</sup>

We found that atrophy in patients with PMD0-1 affects the corpus callosum, a pure white matter myelinated anatomic neuron body-free structure. This is in agreement with Laukka et al., suggesting a link between clinical severity and abnormal corpus callosum development.<sup>9</sup> We also found intra-individual change in atrophy over time, which would make the corpus callosum a potentially good morphological marker both for motor development and for disease progression with age. Corpus callosum atrophy of the most severe patients is also suggestive of global white matter loss in patients with PMD/SPG2.<sup>9</sup> However, we were unable to find a correlation between MDS and white matter fraction despite a segmentation of 43% of the MRI, including all groups of patients. This might be because of the sample size. FLAIR sequences on MRI were well contrasted in all patients. The difficulties to segment white matter using SPM were more related to the quality of the FLAIR sequences during the MRI acquisition, particularly because of artefact movements of the head in link with patients' ataxia. Laukka et al.<sup>9</sup> also struggled with automated segmentation in patients with PMD and so had to perform meticulous manual segmentation of the white matter, which might be particularly impracticable in routine. Another hypothesis would be that proportions of white matter and grey matter compartments remain stable whatever the global brain atrophy, suggesting a mechanism of both neuronal and myelin atrophy in PMD/SPG2. This hypothesis is coherent with neuropathological data in patients with PMD/SPG2,<sup>15</sup> clinical data in patients with SPG2 with length-dependent axonal degeneration,<sup>16</sup> and data in animal models<sup>17,18</sup> that have already shown a clear involvement of neurons in the physiopathology of PLP1-related disorders. It has been suggested that the underlying process could be a secondary axonal suffering<sup>19</sup> or a direct neuronal PLP1 pathological expression in neurons.<sup>20,21</sup> Two patients had an apparent loss of white matter after 15 years of age. This white matter loss was simultaneously associated with severe global atrophy, severe corpus callosum atrophy, and a mild increase in global and cerebellar atrophy over time. This result suggests there could be a delay in global white matter atrophy compared with the corpus callosum atrophy. The corpus callosum is known to be an early myelinated and very compacted structure. Global white matter atrophy may follow the corpus callosum atrophy in the time-course of the disease.

The absence of correlation between cerebellum volume and developmental score in our series argues against the cerebellum as a biomarker for motor development. However, cerebellum atrophy has been reported in severe PMD.<sup>16</sup> In addition, neuronal loss affecting particularly thalamic, hippocampal, and cerebellar neurons (Purkinje cells and neurons of the dentate nuclei) was reported on brain examination in different forms of PMD/SPG2, suggesting that

cerebellum atrophy would be caused not only by white matter injury but also by grey matter loss.<sup>15</sup>

Nevertheless, we found that cerebellum atrophy could increase over time. Interestingly, cerebellum volume decreased not only in an inter-individual manner from 5 years old but also in an intra-individual manner on the MRI follow-up. A recent study in children with typical development reported that cerebellum volume increases until the beginning of adolescence and then tends to decrease slightly thereafter.<sup>22</sup> These results point to cerebellum volume as a good marker for progressive grey matter and white matter injury with age in PMD/SPG2.

We failed to find a relationship between developmental score and global hypomyelination at the first MRI with adjustment to age, even though hypomyelination is the main neuropathological feature in PMD<sup>15</sup> and orientates the diagnosis on cerebral MRI.<sup>2</sup> This lack of relationship may be because of lack of power in our study, but either way, this putative link remains controversial.<sup>4–6</sup> Nevertheless, hypomyelination of frontal white matter, anterior limb of the internal capsule, and arcuate fibres was correlated to MDS, showing that the most anterior and late-myelinated regions are more affected in PMD/SPG2. Furthermore, intra-individual MRI follow-up revealed slight myelination progression until 12 years in five patients with classical and mild PMD, whereas no progression was observed in older patients. To confirm myelination progression in the earliest MRIs, we also analysed MRIs performed before (n=10 patients) and later than (n=7 patients) our study in patients including all severity scores (Fig. S1). We again found a slow progression of myelination until 12 years even in the most severe patients, whereas there was no global change in myelination in older patients. These findings are in agreement with MRI data already reported in young patients with classical and mild PMD.<sup>6</sup> This spontaneous progression of myelination during the first years of life might be of utmost importance for future therapeutic trials. For instance, the interpretation of patchy progression of brain myelination in young patients with PMD after local injections of neural stem cells warrants extreme caution.<sup>7</sup>

In conclusion, this study highlights that not just hypomyelination but also brain atrophy are major features on MRI in PMD/SPG2. Myelination progression may be informative during the early years of life, but motor development score was more correlated to markers of atrophy. Corpus callosum and cerebellum volumes may be good intra-individual markers of disease progression with age.

These findings could well be important for PMD/SPG2 patient follow-up in future therapeutic trials.



## ACKNOWLEDGEMENTS

The authors thank the members of the Leukotreat European Consortium. The authors have stated that they had no interests that might be perceived as posing a conflict or bias.

## SUPPORTING INFORMATION

The following additional material may be found online:

*Table S1:* Additional results of statistical analyses for the different biomarkers.

*Figure S1:* Evolution of myelination score in PMD and SPG2 patients considering previous and later MRI.

## References

1. Cailloux F, Gauthier-Barichard F, Mimault C, et al. Genotype-phenotype correlation in inherited brain myelination defects due to proteolipid protein gene mutations. *Clinical European Network on Brain Dysmyelinating Disease. Eur J Hum Genet* 2000; 8: 837–45.
2. Steenweg ME, Vanderver A, Blaser S, et al. Magnetic resonance imaging pattern recognition in hypomyelinating disorders. *Brain* 2010; 133: 2971–82.
3. van der Knaap MS, Valk J. Myelination and retarded myelination. In: van der Knaap MS, Valk J, editors. *Magnetic Resonance of Myelin, Myelination, and Myelin Disorders*. Berlin: Springer-Verlag, 1995: 31–52.
4. Nezu A, Kimura S, Takeshita S, et al. An MRI and MRS study of Pelizaeus-Merzbacher disease. *Pediatr Neurol* 1998; 18: 334–37.
5. Takanashi J, Sugita K, Tanabe Y, et al. MR-revealed myelination in the cerebral corticospinal tract as a marker for Pelizaeus-Merzbacher's disease with proteolipid protein gene duplication. *Am J Neuroradiol* 1999; 20: 1822–28.
6. Plecko B, Stockler-Ipsiroglu S, Gruber S, et al. Degree of hypomyelination and magnetic resonance spectroscopy findings in patients with Pelizaeus-Merzbacher phenotype. *Neuropediatrics* 2003; 34: 127–36.
7. Gupta N, Henry RG, Strober J, et al. Neural stem cell engraftment and myelination in the human brain. *Sci Transl Med* 2012; 4: 155ra137.
8. Boespflug-Tanguy O, Labauge P, Fogli A, Vauras-Barriere C. Genes involved in leukodystrophies: a glance at glial functions. *Curr Neurol Neurosci Rep* 2008; 8: 217–29.
9. Laukka JJ, Stanley JA, Garbern JY, et al. Neuroradiologic correlates of clinical disability and progression in the X-linked leukodystrophy Pelizaeus-Merzbacher disease. *J Neurol Sci* 2013; 335: 75–81.
10. Inoue K. PLP1-related inherited dysmyelinating disorders: Pelizaeus-Merzbacher disease and spastic paraplegia type 2. *Neurogenetics* 2005; 6: 1–16.
11. Rothman KJ. No adjustments are needed for multiple comparisons. *Epidemiology* 1990; 1: 43–46.
12. Feise RJ. Do multiple outcome measures require p-value adjustment? *BMC Med Res Methodol* 2002; 2: 8.
13. Wang PJ, Young C, Liu HM, et al. Neurophysiologic studies and MRI in Pelizaeus-Merzbacher disease: comparison of classic and congenital forms. *Pediatr Neurol* 1995; 12: 47–53.
14. Biancheri R, Grossi S, Regis S, et al. Further genotype-phenotype correlation emerging from two families with PLP1 exon 4 skipping. *Clin Genet* 2014; 85: 267–72.

15. Sima AA, Pierson CR, Woltjer RL, et al. Neuronal loss in Pelizaeus-Merzbacher disease differs in various mutations of the proteolipid protein 1. *Acta Neuropathol* 2009; 118: 531–39.
16. Garbern JY, Yool DA, Moore GJ, et al. Patients lacking the major CNS myelin protein, proteolipid protein 1, develop length-dependent axonal degeneration in the absence of demyelination and inflammation. *Brain* 2002; 125: 551–61.
17. Miller MJ, Haxhiu MA, Georgiadis P, et al. Proteolipid protein gene mutation induces altered ventilatory response to hypoxia in the myelin-deficient rat. *J Neurosci* 2003; 23: 2265–73.
18. McLaughlin M, Barrie JA, Karim S, et al. Processing of PLP in a model of Pelizaeus-Merzbacher disease/SPG2 due to the rumpshaker mutation. *Glia* 2006; 53: 715–22.
19. Anderson TJ, Schneider A, Barrie JA, et al. Late-onset neurodegeneration in mice with increased dosage of the proteolipid protein gene. *J Comp Neurol* 1998; 394: 506–19.
20. Bongarzone ER, Campagnoni CW, Kampf K, et al. Identification of a new exon in the myelin proteolipid protein gene encoding novel protein isoforms that are restricted to the somata of oligodendrocytes and neurons. *J Neurosci* 1999; 19: 8349–57.
21. Sarret C, Combes P, Micheau P, et al. Novel neuronal proteolipid protein isoforms encoded by the human myelin proteolipid protein 1 gene. *Neuroscience* 2010; 166: 522–38.
22. Kosar MI, Karacan K, Otag I, et al. Determination of cerebellar volume in children and adolescents with magnetic resonance images. *Folia Morphol* 2012; 71: 65–70.